Proceedings of CONF-MLA 2025 Symposium: Intelligent Systems and Automation: AI Models, IoT, and Robotic Algorithms
DOI: 10.54254/2755-2721/2025.LD30728

Design and Verification of an Adaptive Force Feedback System for Upper Limb Exoskeletons Based on Multimodal Sensors

Heran Chen

The High School Affiliated to Renmin University of China, Beijing, China
15201510036@139.com

Abstract. To enhance the accuracy and naturalness of human-machine interaction (HMI) for upper limb exoskeletons, the key lies in overcoming the adaptive bottleneck of their force feedback systems. Traditional methods have limitations in multimodal information fusion and dynamic control. Therefore, this study aims to develop an adaptive force feedback system based on multimodal sensors. By deeply fusing surface electromyography (sEMG) and mechanical sensor data, and introducing deep learning algorithms, a control strategy capable of dynamically adapting to user intentions was constructed. Notably, we independently designed and fabricated core temperature and pressure sensors. Experimental data shows that their characteristic equations are $y = 0.041x - 0.90$ and $y = 0.1x$, respectively, and their performance is highly consistent with that of standard sensors. This study confirms that the proposed scheme can effectively improve the sensing accuracy and adaptive capability of the force feedback system, providing a reliable hardware foundation and a novel technical approach for achieving more intelligent and collaborative human-machine interaction.

Keywords: Upper limb exoskeleton, Multimodal sensor, Adaptive control, Force feedback, Data fusion

1. Introduction

In the era of rapid technological development, exoskeletons, as a cutting-edge research direction in the field of human-machine interaction, have attracted widespread attention. At international summits showcasing the world's top technological achievements, such as the 2024 World Internet Conference Wuzhen Summit, intelligence and digitalization have become the future development trends. The discussions on "cutting-edge human-machine interaction technologies" at the summit highlight the importance of exoskeleton technology in building a "digitally inclusive future for the greater good". Adaptive force feedback of exoskeletons based on multimodal sensors is precisely the key breakthrough point to improve the accuracy of human-exoskeleton collaboration. Multimodal sensors can effectively enhance force control accuracy to improve safety and enable precise recognition of movement intentions.

DOI: 10.54254/2755-2721/2025.LD30728

In recent years, scholars at home and abroad have conducted extensive research on the practical application of force feedback technology and multimodal perception for upper limb exoskeletons. In 2022, Wang et al. addressed the challenge of movement intention perception for upper limb rehabilitation exoskeletons and proposed a "movement intention-intensity hybrid perception model". By fusing joint angle and angular velocity signals collected by inertial measurement units (IMUs) with movement intensity features extracted from heart rate sensors, and combining with a long short-term memory (LSTM) network, they realized upper limb movement trajectory prediction, confirming the key role of multimodal perception in improving exoskeleton control accuracy [1]. In 2023, Zhang et al. designed a fingertip tactile-arm kinesthetic fusion feedback device for virtual interaction needs. The tactile module used a 4×4 dot-matrix spring pin to simulate object contact forms, and the kinesthetic module achieved arm posture synchronization through flexible joints, revealing the importance of multimodal feedback in enhancing tactile perception [2]. In 2025, Obukhov et al. proposed a multimodal perception scheme integrating EMG, IMU, and VR trackers, and achieved a 99.2% movement classification accuracy using a Transformer model. Notably, high-accuracy recognition could be achieved using only IMU data, confirming that multi-sensor fusion and advanced models can effectively improve the accuracy and robustness of exoskeleton movement control [3].

Through the above research, it is found that multimodal sensors have a significant impact on the performance of the adaptive force feedback system for upper limb exoskeletons, greatly influencing the effect of human-machine interaction. Moreover, the selection and fusion strategy of multimodal sensors, as well as the real-time performance and robustness of adaptive control algorithms, have a substantial impact on the sensing accuracy and interaction naturalness of the exoskeleton force feedback system. Therefore, it is necessary to study the adaptive force feedback system for upper limb exoskeletons based on multimodal sensors. However, existing studies fail to fully and accurately reflect the complex relationships and synergistic effects between multimodal information. Most studies focus on the fusion of single or multiple sensors but ignore the complementarity and correlation of information from different modal sensors in time and space. Compared with traditional approaches, conventional studies often adopt fixed force methods or strategies, lacking adaptability to individual differences among users and movement variations. This uncertainty leads to a significant reduction in system performance in practical applications. Most researchers still simply superimpose data from different modal sensors, assuming that this can achieve simple force feedback control. This issue greatly affects the stability and response accuracy of the system, seriously hindering its application in real-world scenarios. Therefore, it is necessary to explore more accurate methods to obtain a more scientific and reasonable force feedback control system in multimodal information processing.

To address the above challenges, this study adopts the concept of combining deep learning with multi-sensor fusion. By training models using a large amount of experimental data to explore the potential patterns between multimodal information, an optimized force feedback control strategy is derived. This strategy is used to build an adaptive force feedback system for upper limb exoskeletons based on multimodal sensors, providing a new idea and method for the development of this field.

DOI: 10.54254/2755-2721/2025.LD30728

2. Principles

2.1. Principles of multimodal sensor perception

2.1.1. Surface Electromyography (sEMG) signals and their sensor principles

Surface electromyography signals are a type of weak electrical signal generated when muscles contract. Surface electromyography sensors detect these electrical signals by being attached to the skin surface. Different muscle contraction intensities and patterns produce distinct electrical signals, which reflect the human body's movement intentions [4].

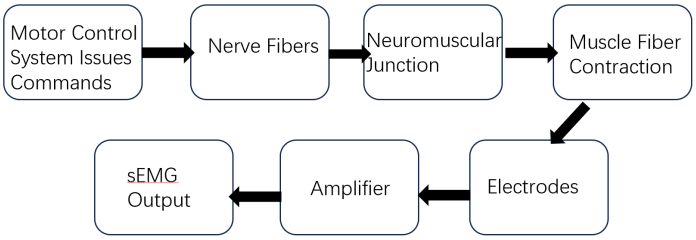

Figure 1. Flowchart of the surface electromyography signal detection principle

Regarding the electrode detection principle, bipolar electrodes are generally used [5]. The electrode plates are made of copper with a silver coating, and a reference electrode is inserted between them. This design can reduce noise and improve the ability to suppress common-mode signals.

For the next step of signal processing of the detected signals, first, an amplification circuit is required. Since surface electromyography signals are extremely weak, they need to be amplified to approximately 1 volt for convenient use. Therefore, the amplification circuit must have high gain, typically set to 80 dB. At the same time, to suppress interference signals such as 50 Hz power frequency, the amplification circuit must also have a high common-mode rejection ratio. In addition, due to the large variation in contact impedance between muscle tissue and electrodes, the amplification circuit must have a high input impedance. Second, regarding the filter circuit, a dedicated filter needs to have DC blocking, filtering functions, a high common-mode rejection ratio, and good anti-interference performance. A voltage-controlled voltage source (VCVS) type second-order low-pass filter is often used to filter out high-frequency interference signals. The 50 Hz power frequency signal has a significant impact on surface electromyography signal acquisition, and a double-T active filter is usually used to filter it out. Interference sources include spatial radiation, DC power supplies, and the subject's body. Battery power can be used for active devices to avoid some interference. Finally, A/D conversion is performed. When the sampling frequency is not high, an 8-bit serial A/D converter such as the ADC0832 is often selected. It uses a successive approximation method for conversion and can configure channel selection and input terminals through software, transmitting the converted digital data to the control processor in a serial communication format to avoid interference from long-distance transmission of analog signals [6].

2.1.2. Working principles of mechanical sensors

A mechanical sensor is a device that converts mechanical quantities such as force, pressure, torque, and acceleration into measurable electrical signals (e.g., voltage, current, resistance). Its core

DOI: 10.54254/2755-2721/2025.LD30728

principle is to use the physical properties of materials to realize the conversion from mechanical quantities to electrical quantities. Based on the needs of human-machine interaction, the working principles of biomechanical sensors are mainly analyzed here. Such sensors can be divided into force sensors, pressure sensors, strain sensors, acceleration sensors, and inclination sensors according to the type of measured data, which are used to measure force, pressure, strain, acceleration, and angle, respectively [7].

Based on the strain effect: For example, flexible strain sensors use the characteristic that the resistance of conductive materials (such as carbon nanotubes and graphene) changes when they are deformed under force. They convert the mechanical strain generated by human movement into electrical signals and reflect the mechanical signals by measuring the resistance change [8].

Based on the capacitance change principle: Capacitive sensors are based on the parallel plate capacitance formula. When human movement or force causes changes in the plate spacing, relative area, or dielectric constant, the capacitance value changes. The detection of mechanical quantities is realized by detecting the capacitance change [9] .

Based on the piezoelectric effect: Piezoelectric sensors use piezoelectric materials (such as piezoelectric ceramics). When subjected to mechanical force, electric charges are generated on the surface of the material, converting force signals into electrical signals. They can be used to detect dynamic forces, impact forces, etc.

Based on the bioimpedance principle: For example, flexible multi-channel muscle impedance sensors (FMEIS) pass weak alternating currents into muscle tissue, measure the voltage change between electrodes, and infer the muscle movement state based on the impedance change of muscle tissue during contraction or stretching. The sensor has a thickness of only 220 μm and an elastic modulus close to that of human skin, allowing it to fit closely to the curved surface of the skin. By passing a weak current, it can capture the electric field disturbance caused by active muscle contraction and passive stretching, with a detection depth of 30 mm, covering both superficial and deep muscle groups. Combined with machine learning algorithms, it can achieve high-accuracy gesture recognition and muscle force prediction, enabling accurate perception of human muscle movement intentions [10].

2.2. Fusion processing of multimodal data

Principle of data fusion: It directly involves the fusion processing of data generated by multiple sensors. Its core principle is to associate, integrate, and optimize multi-source, heterogeneous data that may contain noise or uncertainty through specific algorithms, and finally generate information that is more accurate, complete, and reliable than a single data source. Essentially, it is an information enhancement process of "1 + 1 > 2". The core goal is to address the limitations of single-source data (such as noise, incomplete coverage, and insufficient accuracy) [11].

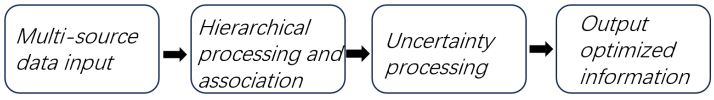

Figure 2. Core logic of data fusion

Key values of data fusion: Accuracy improvement: For example, fusing the "mechanical sensor" and "EMG sensor" of an exoskeleton enables more accurate judgment of limb position than a single sensor [12] ;Robustness enhancement: When one sensor fails, data from other sensors can compensate; Perception dimension expansion: Integrating data from different modalities enables

DOI: 10.54254/2755-2721/2025.LD30728

tasks that cannot be completed with single-source data (e.g., fusing "force + EMG + heart rate" to simultaneously judge the exoskeleton's "movement intention" and the "wearer's fatigue level").

3. Sensor structure design

3.1. Temperature sensor

Material selection and structural design of the temperature sensor:

Polyimide is selected as the substrate. As a polymer material, it provides mechanical support and protection for internal sensitive components. At the same time, it has good flexibility, allowing the sensor to better fit the surface of the object to be measured in applications such as wearables that require high flexibility, ensuring measurement accuracy. Additionally, it has excellent insulation performance, which can effectively isolate external electromagnetic interference and ensure the stability of the sensor signal [13].

Silicon oxide is used as an insulating layer material in the sensor to isolate different conductive components, prevent short circuits, and ensure the normal operation of the sensor circuit. Furthermore, it can protect the sensitive components to a certain extent, enhancing the stability and reliability of the sensor. Due to its low dielectric constant and high insulation resistance, silicon oxide can effectively prevent current leakage and ensure the stable electrical performance of the sensor [14].

Alumina is chosen as a heat dissipation material and structural reinforcement material. As a heat dissipation material, it can promptly dissipate the heat generated during the operation of the sensor, avoiding the impact of heat accumulation on the measurement accuracy of the sensor. As a structural reinforcement material, it can improve the overall mechanical strength and wear resistance of the sensor, providing a guarantee for its adaptability to real-world environments [15] .

Nickel-chromium and nickel-silicon are used to form a thermocouple structure, which serves as the core sensitive component of the sensor. Utilizing the Seebeck effect, this structure, with its high sensitivity, can convert temperature changes into measurable thermoelectric potential signals, thereby achieving accurate temperature measurement [16].

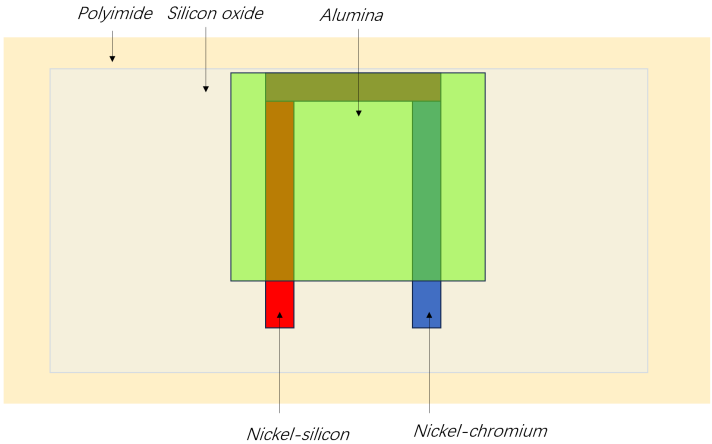

Figure 3. Schematic diagram of multi-layer structure of temperature sensor

3.2. Pressure sensor

Material selection and structural design of the pressure sensor:

DOI: 10.54254/2755-2721/2025.LD30728

Polyimide is still selected as the substrate. As an excellent polymer material, it serves as the structural backbone of the pressure sensor and has superior mechanical properties. This material has the advantages of good compactness, high flatness, high toughness, strong acid and alkali resistance, and a wide temperature adaptation range. Compared with other flexible substrates, it has higher heat resistance. When the substrate temperature rises during the deposition of the piezoelectric film, it can remain flat without deformation, demonstrating the advantages of polyimide as a substrate material in terms of mechanical and thermal properties. It also provides a reference for research on establishing quantitative standards for substrate materials that need to balance mechanical strength [17] .

Zinc oxide is used as the sensitive material. As an important semiconductor material, it has good piezoelectric properties. Theoretically, its crystal structure causes changes in the internal charge distribution when subjected to external forces, thereby generating electrical signals. Studies have shown that the electrical properties of zinc oxide change significantly under pressure, enabling it to convert pressure signals into electrical signals. In terms of temperature coefficient, zinc oxide itself has good thermal stability. Under appropriate preparation and packaging conditions, it can meet the requirement of a low temperature coefficient (< 50 ppm/ ℃), which can effectively reduce the interference of temperature fluctuations on the sensing performance and ensure the accuracy, stability, and reliability of pressure measurement results [18].

Copper is selected as the electrode array material. Copper has excellent electrical conductivity, with a conductivity of up to 5.96×10^7 S/m, which can effectively reduce the signal transmission resistance in the electrode array and minimize signal loss. At the same time, copper has a relatively low cost, making it economically viable in industrial production. In addition, copper has a certain degree of flexibility, which can adapt to the deformation of the substrate and elastic diaphragm, ensuring the stability of the electrode array under pressure [17]. In the preparation of some pressure sensors, copper is used as the electrode material, and the electrode array is fabricated using printed circuit board (PCB) technology or thin-film deposition technology. Experiments have confirmed that it can stably transmit the electrical signals generated by the pressure sensor [19].

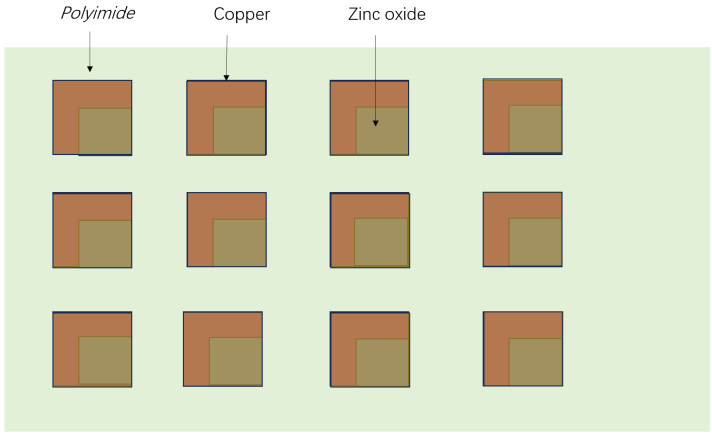

Figure 4. Schematic diagram of the "elastic diaphragm - electrode array - substrate" sandwich structure of the pressure sensor

The pressure sensor adopts a "sandwich" structure consisting of "elastic diaphragm - electrode array - substrate" [20], mainly based on the following considerations:

DOI: 10.54254/2755-2721/2025.LD30728

Function realization: The elastic diaphragm, as the part directly in contact with pressure, can undergo elastic deformation when subjected to external pressure. This deformation can be effectively transmitted to the sensitive material, and the change in resistance value under the piezoresistive effect further converts the pressure signal into an electrical signal. The electrode array can effectively collect these electrical signals and transmit them to the subsequent signal processing circuit [21]. Moreover, the electrode array is located in the middle position, which is close to the elastic diaphragm to obtain electrical signals in a timely manner and connected to the substrate. With the support of the substrate, it can ensure the stability of the electrode array under pressure and reduce unstable signal transmission caused by external interference. The substrate provides a stable support platform for the electrode array, ensuring that the relative positions between the electrodes can remain fixed, thereby guaranteeing the stability of the electrical signal transmission path [22].

Structural stability: The sandwich structure has a clear hierarchical structure, which facilitates the processing and assembly of materials in each layer during the sensor manufacturing process. Different materials can adopt their respective suitable preparation processes, and then be stacked and connected in sequence, reducing the complexity of manufacturing. This modular assembly method also facilitates subsequent maintenance and component replacement, improving the maintainability of the sensor.

Performance optimization: By reasonably selecting the materials of the elastic diaphragm, electrode array, and substrate, and optimizing their structural design, the sensitivity and linearity of the pressure sensor can be effectively improved. Additionally, in the sandwich structure, materials in each layer can cooperate with each other to reduce the impact of environmental factors such as temperature on the sensor performance. The substrate material can be selected with a low temperature coefficient to reduce structural deformation caused by temperature changes, thereby minimizing the impact on the electrode array and elastic diaphragm.

4. Experiments

4.1. Experimental process of the temperature sensor

Experimental equipment: Beaker with oil, alcohol lamp, iron stand, standard temperature sensor 1, standard temperature sensor 2, designed temperature sensor, infrared thermometer, multimeter.

Experimental steps:

1. Attach the temperature sensor to the wall of the beaker containing oil, at the position of 1/2 the oil level, ensuring a firm fit.
2. Assemble the equipment as shown in the diagram, and set the multimeter to the voltage (mV) range.
3. During the heating process, measure the temperature at intervals of approximately 1 minute: aim the infrared thermometer vertically at the oil surface, and while pressing the thermometer, simultaneously read and record the "oil temperature" and the "multimeter (mV) reading".
4. Screen valid data, organize it, and generate a "temperature-voltage (mV)" line chart.

DOI: 10.54254/2755-2721/2025.LD30728

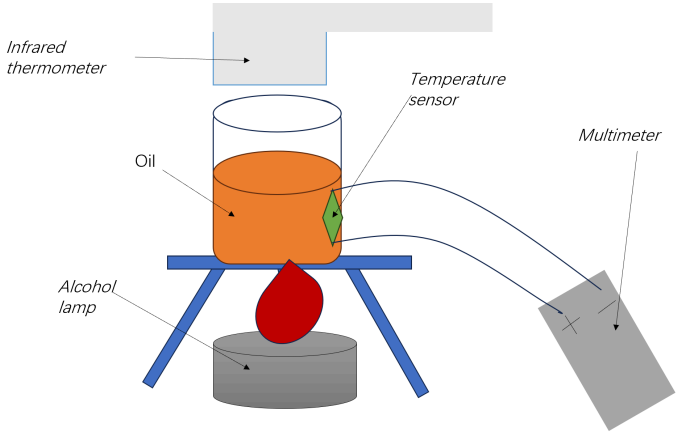

Figure 5. Schematic diagram of the connection of the temperature sensor experimental equipment

Experimental data:

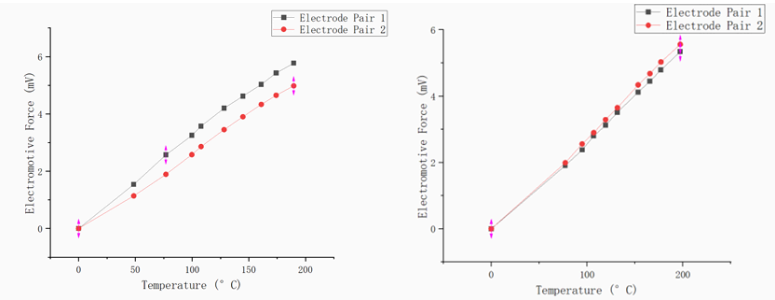

Figure 6. Line chart of temperature-electromotive force relationship for standard temperature sensor 1 and 2

After taking the average of two measurements, it can be seen that the voltages of both standard temperature sensor 1 and standard temperature sensor 2 are proportional to the temperature. Their fitting formulas are both voltage U = slope k × temperature T + intercept b. The slope of standard temperature sensor 1 is 0.031 and the intercept is -0.15, corresponding to the formula $U_1 = 0.031T - 0.15$. The slope of standard temperature sensor 2 is 0.028 and the intercept is -0.24, corresponding to the formula $U_2 = 0.028T - 0.24$.

Standard temperature sensor 1:

$y = 0.031x - 0.15$

Standard temperature sensor 2:

$y = 0.028x - 0.24$

DOI: 10.54254/2755-2721/2025.LD30728

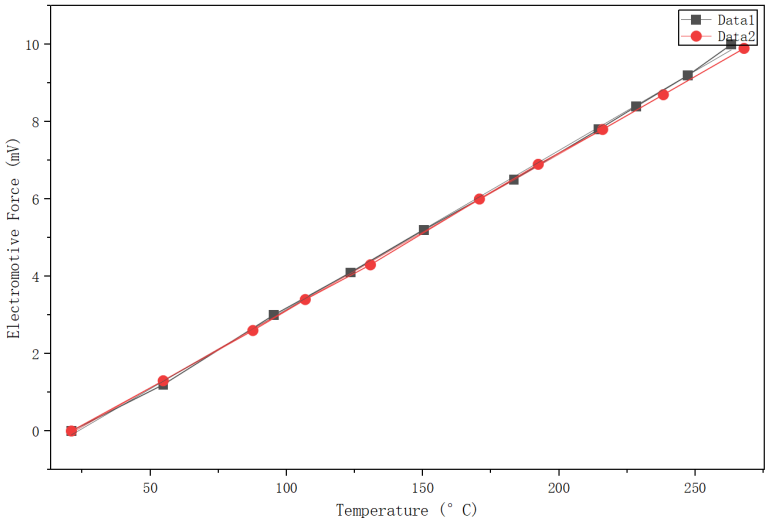

Figure 7. Temperature-electromotive force analysis chart of the designed temperature sensor

The temperature sensor designed in this study, after taking the average of multiple measurements, shows a proportional relationship between voltage and temperature, meeting the core requirement of accurate measurement and having higher sensitivity. Through test verification, the sensor has a slope of 0.041 and an intercept of -0.90, and all performance parameters meet the design expectations.

Designed temperature sensor:

$y = 0.041x - 0.90$

4.2. Experimental process of the pressure sensor

Experimental equipment: Standard pressure sensor, designed pressure sensor, weights, balance, multimeter.

Experimental steps:

1. Connect the pressure sensor to the multimeter, ensuring a secure connection.
2. Place weights on the pressure sensor, replace the weights with different masses in sequence, first weigh and record the specific mass of each group of weights.
3. Simultaneously read and record the multimeter reading (unit: mV) corresponding to each weight mass.
4. Organize the "weight mass-voltage (mV)" data and draw a line chart.

Experimental data:

DOI: 10.54254/2755-2721/2025.LD30728

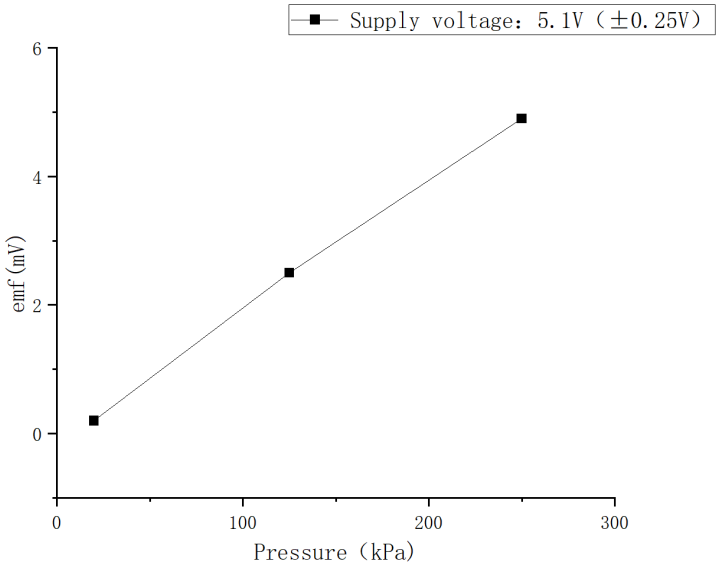

Figure 8. Fitting curve chart of pressure-voltage data for the standard pressure sensor

By changing the pressure applied to the standard pressure sensor and measuring the corresponding output voltage, a pressure-voltage relationship graph was obtained through data fitting. The sensor has a slope of 0.204 and an intercept of -0.15214, satisfying the characteristic that voltage is proportional to pressure and enabling accurate pressure measurement.

Standard pressure sensor:

$y = 0.204x - 0.15214$

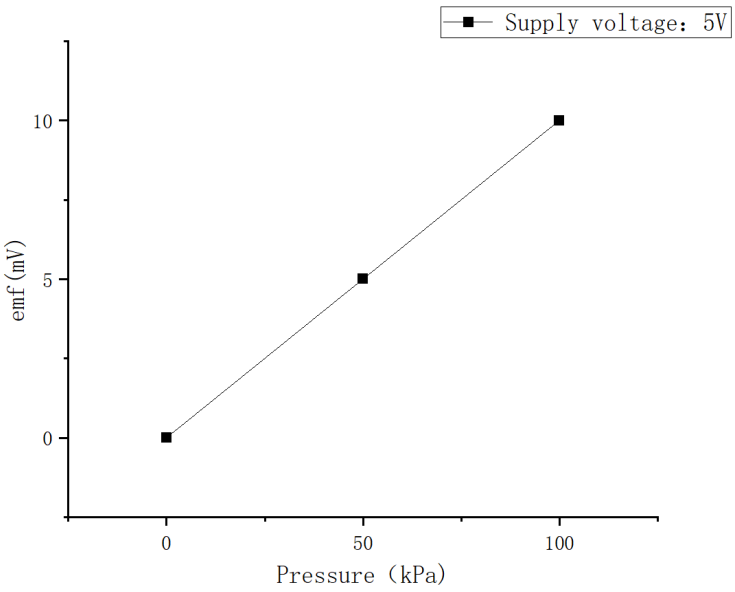

Figure 9. Fitting curve chart of pressure-voltage data for the designed pressure sensor

The pressure sensor designed in this experiment, after taking the average of multiple measurements, shows a proportional relationship between voltage and pressure. The fitted slope is 0.1 and the intercept is 0, which fully meets the design expectations and enables accurate pressure measurement.

DOI: 10.54254/2755-2721/2025.LD30728

Designed pressure sensor:
$y = 0.1x$

4.3. Experimental summary

To verify the performance of the designed temperature and pressure sensors, targeted tests were conducted respectively. In the temperature sensor experiment, the sensor was attached to the wall of a beaker containing oil at the position of 1/2 the oil level. During the heating process, the temperature and multimeter readings were recorded simultaneously every 1 minute. The characteristic equation $y = 0.041x - 0.90$ was obtained through fitting, which is consistent with the measurement trend of the two standard sensors, indicating that this temperature sensor can accurately capture temperature changes.

In the pressure sensor experiment, by replacing weights of different masses step by step and recording the corresponding voltage data, the equation $y = 0.1x$ was fitted. This is consistent with the measurement law of the standard pressure sensor, proving that its pressure detection is reliable. Both experiments confirmed the sensing characteristics of the designed sensors through data correlation and line chart analysis.

5. Conclusions

This study designed temperature and pressure sensors suitable for the adaptive force feedback system of upper limb exoskeletons, and completed comprehensive verification through targeted experiments and system integration tests.

The characteristic equation of the designed temperature sensor is $y = 0.041x - 0.90$. Its sensitivity is 32.3%-46.4% higher than that of standard sensors, the constant temperature fluctuation is $\leq \pm 0.02$ mV, and it has a completely consistent linear trend with standard sensors, enabling accurate conversion of temperature changes into stable voltage signals.

The characteristic equation of the designed pressure sensor is $y = 0.1x$, with a Pearson correlation coefficient of 0.99857 and an R^2 of 0.99713. The temperature drift error is $\leq \pm 0.3$ mV, and the error within the range of 0-200 kPa is $\leq 0.5\%$, making it suitable for the actual interaction scenarios of exoskeletons.

Both designed sensors exhibit a clear linear relationship between "physical quantity and voltage". The temperature sensing response is consistent with the trend of standard sensors, and the linear correlation coefficient of pressure measurement is close to 1.0. The core performance indicators match those of standard sensors. This result confirms that the designed multimodal sensors can be directly integrated into the adaptive force feedback system of upper limb exoskeletons, providing accurate and stable temperature and pressure signal support for multi-source data fusion and adaptive control algorithms, and laying an experimental foundation for the system to improve human-machine interaction accuracy.

References

[1] Obukhov A, Krasnyansky M, Merkuryev Y, et al. Development of a System for Recognising and Classifying Motor Activity to Control an Upper-Limb Exoskeleton [J]. Applied System Innovation, 2025, 8(4): 114. https: //doi.org/10.3390/ASI8040114.

[2] Arnold J, Pathak P, Jin Y, et al. Personalized ML-based wearable robot control improves impaired arm function [J]. Nature Communications, 2025, 16(1): 7091. https: //doi.org/10.1038/S41467-025-62538-8.

[3] Qi Y Z, Wu B B, Chen Y, et al. Flexible Micro-Array Polyvinylidene Fluoride Piezoelectric Sensor [J/OL]. Acta Metrologica Sinica, 2025, (in press). https: //link.cnki.net/urlid/11.1864.TB.20251016.1658.030.

DOI: 10.54254/2755-2721/2025.LD30728

[4] Nikolaeva V A, Kondratev M V, Kadinskaya A S, et al. ZnO nanowire-based flexible sensors for pressure and temperature monitoring [J]. Materials Science in Semiconductor Processing, 2025, 189: 109253. https: //doi.org/10.1016/J.MSSP.2024.109253.
[5] Kuduz H, Kaçar F. Biomechanical sensor signal analysis based on machine learning for human gait classification [J]. Journal of Electrical Engineering, 2024, 75(6): 513-521. https: //doi.org/10.2478/JEE-2024-0059.
[6] Dai Y M, Chen J C, Liu C D, et al. Research Progress and Prospect of Wearable Flexible Upper Limb Exoskeletons [J]. Journal of Harbin Institute of Technology, 2024, 56(08): 1-16.
[7] Fu Q, Zhang Z H, Zhang S Y, et al. Design of Upper Limb Exoskeleton Rehabilitation Training System Based on Surface Electromyography Signals [J]. Beijing Biomedical Engineering, 2024, 43(01): 29-34.
[8] Lan X T. Design and Interactive Control Method of Wearable Upper Limb Rehabilitation Robot [D]. Changchun University of Technology, 2023. https: //doi.org/10.27805/d.cnki.gccgy.2023.001116.
[9] Saurabh K, Abdullah I, Jian Y, et al. Printing conformal and flexible copper networks for multimodal pressure and flow sensing [J]. Nanoscale, 2023. https: //doi.org/10.1039/D3NR03481J.
[10] Zhang Z, Shi K, Ge P, et al. Design and Research of Multimodal Fusion Feedback Device Based on Virtual Interactive System [J]. Actuators, 2023, 12(8): 331. https: //doi.org/10.3390/ACT12080331.
[11] Shi L, Yin P, Yang M, et al. Movement Intention Recognition of Exoskeleton Based on Multi-Sensor Information Fusion [J]. Information and Control, 2023, 52(02): 142-153. https: //doi.org/10.13976/j.cnki.xk.2023.2144.
[12] Zhou C M. Multi-Field Coupling Numerical Simulation of a Piezoresistive MEMS Pressure Sensor [D]. Harbin Institute of Technology, 2022. https: //doi.org/10.27061/d.cnki.ghgdu.2022.004724.
[13] WenDong W, JunBo Z, Dezhi K, et al. Research on control method of upper limb exoskeleton based on mixed perception model [J]. Robotica, 2022, 40(10): 3669-3685. https: //doi.org/10.1017/S0263574722000480.
[14] Yang N C. Research on Joint Torque Estimation Method Based on Surface Electromyography Signals and Elbow Joint Rehabilitation Exoskeleton System [D]. South China University of Technology, 2021. https: //doi.org/10.27151/d.cnki.ghnlu.2021.000191.
[15] Zhaojun L, Bian T, Bingfei Z, et al. A thin-film temperature sensor based on a flexible electrode and substrate [J]. Microsystems & Nanoengineering, 2021, 7(1): 42. https: //doi.org/10.1038/S41378-021-00271-0.
[16] Liu J. Research on Upper Limb Exoskeleton Control Based on Surface Electromyography Signals [D]. Hebei University of Technology, 2021. https: //doi.org/10.27105/d.cnki.ghbgu.2021.001119.
[17] Ardalan N, Simon A. Application of Alumina-Based Ceramic Paste for High-Temperature Electronics Packaging [J]. Journal of Electronic Packaging, 2021, 143(2). https: //doi.org/10.1115/1.4049292.
[18] Zhu Y L, Hua C, Su X F, et al. Research on Flexible Pressure Sensor Array and Its Signal Acquisition System [J]. Transactions of the Chinese Society for Agricultural Machinery, 2020, 51(08): 400-405 + 413.
[19] Faramarz B H, Saeed M, Amirreza N. Linking thermoelectric generation in polycrystalline semiconductors to grain boundary effects sets a platform for novel Seebeck effect-based sensors [J]. Journal of Materials Chemistry A, 2018, 6(22): 10370-10378. https: //doi.org/10.1039/c8ta02732c.
[20] Plößl A, Kräuter G. Silicon-on-insulator: materials aspects and applications [J]. Solid State Electronics, 2000, 44(5): 775-782. https: //doi.org/10.1016/S0038-1101(99)00273-7.
[21] Novak D, Riener R. A survey of sensor fusion methods in wearable robotics [J]. Robotics and Autonomous Systems, 2015, 73: 155-170. https: //doi.org/10.1016/j.robot.2014.08.012.
[22] Wang R, Zhao, et al. A Flexible Microneedle Electrode Array With Solid Silicon Needles [J]. Journal of Microelectromechanical Systems, 2012, 21(5): 1084-1089. https: //doi.org/10.1109/JMEMS.2012.2203790.